THE JOURNAL OF PHYSICAL CHEMISTRY B

Article

pubs.acs.org/JPCB

Ion Pairing and Anion-Driven Aggregation of an Ionic Liquid in Aqueous Salt Solutions

Ines F. Pierola* and Yahya Agzenai

Departamento de Ciencias y Técnicas Fisicoquímicas, Facultad de Ciencias, Universidad a Distancia (UNED), 28040 Madrid, Spain

ABSTRACT: A relevant question regarding ionic liquids is whether they exist in aqueous solution as totally dissociated ions or as ionic pairs, molecularly dispersed or forming part of aggregates. Several methods were employed here to evaluate these points by comparing the results of an ionic liquid, 1-ethyl-3-methylimidazolium tosylate ([emim][TOS]) with its model compound *p*-toluenesulfonic acid (pTSA). Conductivity measurements of [emim][TOS] and pTSA dissolved in deionized water support the existence of small amounts of aggregates for both compounds, with a larger extent in the first case. However, apparent molar volume measurements provide no clear evidence for aggregation in aqueous solution or in NaCl aqueous solutions. In contrast, the excimer emission and the absorption and excitation spectra prove the existence of aggregates of [emim][TOS] and pTSA anions in aqueous solution, with and without salt, giving in addition structural information about them. It was thus found that only [emim][TOS] forms ion pairs in deionized water, which dissociate in the presence of NaCl. J-aggregates of pTSA and [emim][TOS] anions, with slip angles that decrease with increasing concentration, were observed through the excitation spectra, and the roles of the anion and cation as well as the effect of the presence of NaCl were analyzed. Thanks to aggregation-induced emission enhancement, fluorescence is much more sensitive than conductivity or density measurements to detect aggregation.

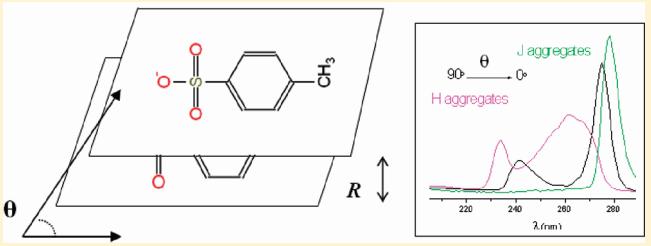

INTRODUCTION

Ionic liquids (ILs) are a novel class of soft materials with interesting properties that are driving new applications in several fields.[1] In general, ILs are organic salts whose melting points are below or around room temperature. Despite the large amount of data recently published, there is not enough information on the structure of ILs in the neat or dissolved state, which is important in understanding their role in practical applications. ILs form solvent-dependent aggregates which may be small clusters, micelles, or long-range ordering of particles as those for surfactants. Ionic association was proposed to explain the self-diffusion coefficients of cations and anions in neat ILs.[2] The aggregation behavior of several ILs in aqueous solution was mainly studied from the point of view of the influence of the cation structure, which is usually modified through changes of the alkyl chain length of the ring substituents and the type of ring.[3−10] The critical aggregation concentration (cac) as well as the critical micelle concentration (cmc) was determined through abrupt changes of some property, namely, the surface tension, ionic conductivity, or apparent molar volume.[3,4] Fluorescence spectroscopy was also employed to determine the aggregation number and cac values of a number of ILs in aqueous solution.[3,6,8]

Fluorescence studies on ILs have been performed by means of fluorescent probes or labels and making use of their intrinsic fluorescence. Imidazolium-based ILs that incorporate carbazole, anthracene, or trimethylphenyl moieties in the cation demonstrated strong and stable intrinsic fluorescence.[9,11,12] The imidazolium group itself shows intrinsic fluorescence that is generally weak and strongly dependent on the excitation wavelength,[6,13,14] whereas it is very intense when the imidazolium group is symmetrical, as for 1,3-dibutylimidazolium chloride.[15] The intrinsic fluorescence of the IL 1-ethyl-3-methylimidazolium tosylate ([emim][TOS], Scheme 1) bearing a fluorescent anion (*p*-toluenesulfonate, also called tosylate) was also reported.[16] In this work, we use the intrinsic fluorescence of tosylate together with conductivity and molar volume measurements to give out information on the structure of the IL [emim][TOS] and its model compound, *p*-toluenesulfonic acid (pTSA), in aqueous media. The details of the structure considered here include the formation of ionic pairs and aggregation.

Scheme 1. 1-Ethyl-3-methylimidazolium Tosylate ([emim][TOS])

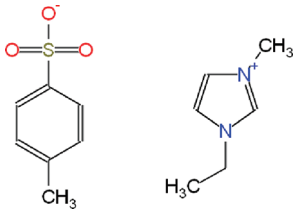

Salt effects are important in systems where electrostatic and hydrophobic interactions are present, as for ILs in aqueous

Received: December 18, 2011
Revised: March 12, 2012
Published: March 15, 2012

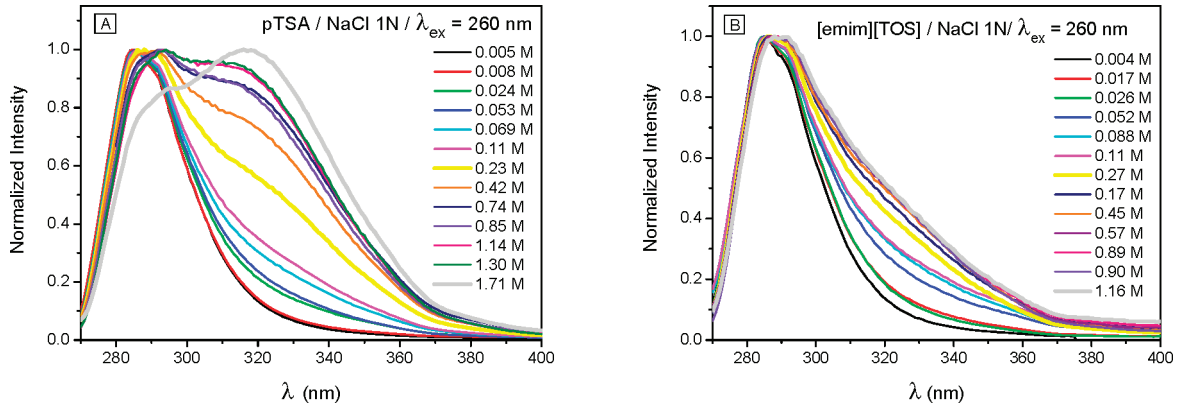

Figure 1. Normalized fluorescence spectra of (A) pTSA, and (B) [emim][TOS], dissolved in 1 N NaCl aqueous solution with chromophore concentrations indicated in the inserts. Excitation wavelength 260 nm.

solution. Depending on the IL and salt, salting-in or salting-out effects were observed. The aqueous solubility of some ILs exhibits salting-in effects that were ascribed to the existence of preferential specific interactions between the apolar moiety of the IL and the ions of the inorganic salts.[17] Salting-out effects on the aggregation of some IL in aqueous solution were also observed.[18] On the other hand, the ionic strength afforded by the inorganic salt is expected to shield ion−ion interactions of the IL. Here we study the structures of the IL and its model compound in NaCl aqueous solutions in order to compare them with those in deionized water.

■ EXPERIMENTAL SECTION

1-Ethyl-3-methylimidazolium tosylate (degree of purity 99.5 to 99.8%, depending on the lot, as measured by means of HPLC or Kjeldahl titration, by the supplier) and *p*-toluenesulfonic acid monohydrate (ACS reagent, purity specification ≥98.5%) were purchased from Fluka and Sigma-Aldrich, respectively. ^{1}H NMR measurements of D_2O solutions, carried out in a Bruker DRX 400 spectrometer, show no impurity above the detection limit. Both compounds were used without further purification. Deionized water (Milli-Q system from Millipore) and standard NaCl aqueous solutions 1.0 N (Fluka) and 0.1033 N (Sigma-Aldrich) were used as solvents. Solutions of [emim][TOS] or pTSA were prepared by mass, and molar concentrations were calculated using the measured values of the density.

Absorption spectra were measured with a Perkin-Elmer Lambda 6 UV/vis spectrophotometer. The absorption spectra of the most concentrated solutions were observed with 4 mm optical path quartz cuvettes, while 1 cm quartz cuvettes were employed for the dilute solutions. The molar extinction coefficient of tosylate at 260 nm is as follows: 301 $L{\cdot}mol^{-1}{\cdot}cm^{-1}$ for [emim][TOS] in dilute aqueous solution and 326 or 335 $L{\cdot}mol^{-1}{\cdot}cm^{-1}$ for pTSA or [emim][TOS] in 1.0 N NaCl aqueous solution.

Steady-state excitation and emission spectra were measured in an SLM-Aminco Bowman AB2 spectrometer. The transmission configuration with the standard right-angle excitation−emission geometry was employed for dilute solutions (chromophore concentrations in the range 1×10^{-4} to 1×10^{-2} M) while the front face configuration was used for chromophore concentrations in the range 1×10^{-3} to 3 M, in order to avoid filter effects and reabsorption of the emission. An incident angle of 21° was employed in the front face configuration to prevent the incident light being reflected in the direction of the observed emission. The excitation and emission bandpasses were kept at 4 nm. The excitation wavelengths (λ_{ex}) employed for emission were in the range 230−275 nm and the emission wavelengths (λ_{em}) for excitation spectra were 290−340 nm. The excimer-to-monomer fluorescence ratio (I_E/I_M) of the emission spectra was determined as the ratio of the intensities at 320 nm (excimer emission, I_E) and 286 nm (monomer emission, I_M) measured with respect to the baseline at 400 nm, minus the ratio of the intensities at 320 and 286 nm of the pure monomer emission band, measured at concentrations in the range 10^{-4} M. Solutions were filtered prior measurements, except when indicated.

The ionic conductivity measurements were carried out at 25.0 °C by means of a Metrohm 712 conductometer at a fixed frequency of 2400 Hz. The sample container was equipped with a water-circulating jacket which allows controlling the temperature within ±0.05 °C. The conductance cell constant was checked with KCl solutions. The conductivity of water, aged as long as the aqueous solutions, was subtracted from the measured data of solutions with very low concentrations.

Density measurements (ρ) were performed with an Anton Paar DMA4500 vibrating-tube digital densitometer at 25.00 °C. The temperature was controlled automatically by the densitometer within 0.005 °C, and the estimated uncertainty in the density is 1×10^{-5} $g{\cdot}cm^{-3}$.

■ RESULTS AND DISCUSSION

The experimental results on the emission, absorption, and excitation spectra, the ionic conductivity, and the apparent molar volume, suggest apparently contradictory conclusions on the existence of aggregates of pTSA and [emim][TOS] in aqueous salt solutions. Aggregation-induced emission enhancement makes compatible all the results and provides structural information of the aggregates.

Emission and Absorption Spectra. Fluorescence spectra of pTSA and [emim][TOS] dissolved in deionized water and in NaCl aqueous solutions show monomer and excimer bands[19,20] that overlap partially (Figure 1); the excimer band becomes evident upon subtraction of the emission of very dilute solutions, which corresponds to only monomer emission. The apparent red shift of the monomer emission (285−295 nm with increasing concentration) is due to the increasing relative intensity of the excimer band, which is centered at 319 nm in any case. The proximity of the monomer and excimer bands indicates that the excimer is weakly stabilized with respect to

dx.doi.org/10.1021/jp212202b | J. Phys. Chem. B 2012, 116, 3973−3981

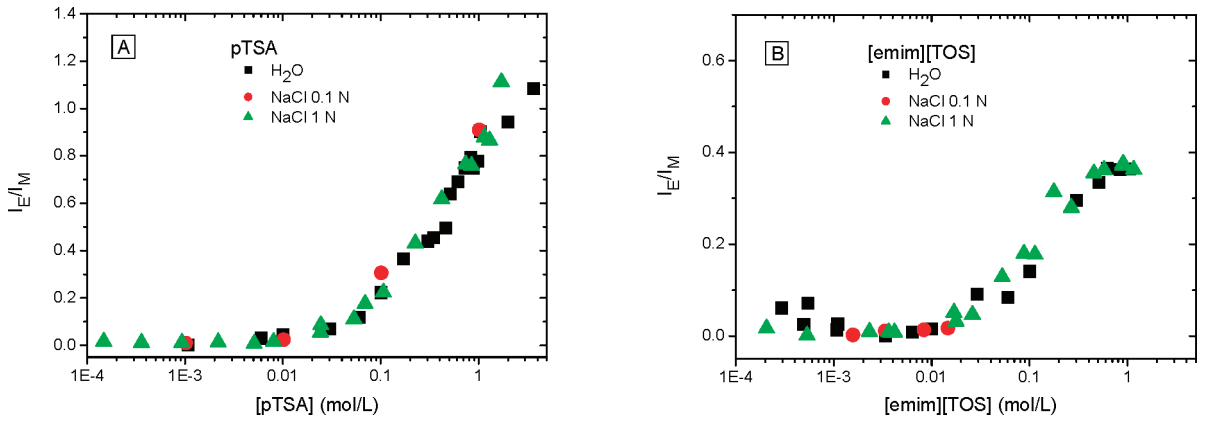

Figure 2. Excimer-to-monomer fluorescence ratio of (A) pTSA and (B) [emim][TOS] dissolved in deionized water and in 0.1 or 1 N NaCl aqueous solutions. Excitation wavelength 260 nm.

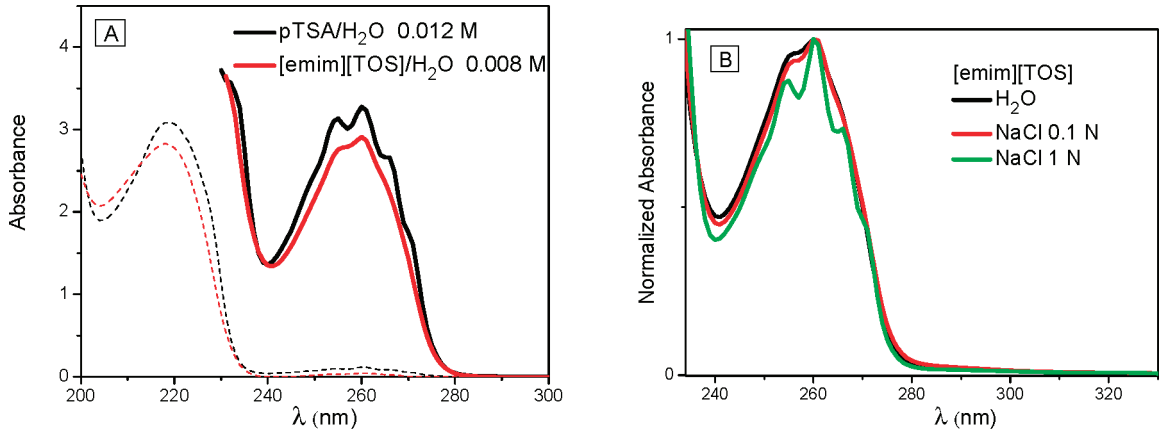

Figure 3. Absorption spectra of (A) pTSA and [emim][TOS] dissolved in deionized water (converted to optical path length 1 cm); the dashed lines correspond to very dilute solutions and show the next absorption band; (B) [emim][TOS] dissolved in deionized water and in 0.1 or 1 N NaCl aqueous solutions with IL concentrations close to 0.01 M (normalized to the maximum absorption at 260 nm).

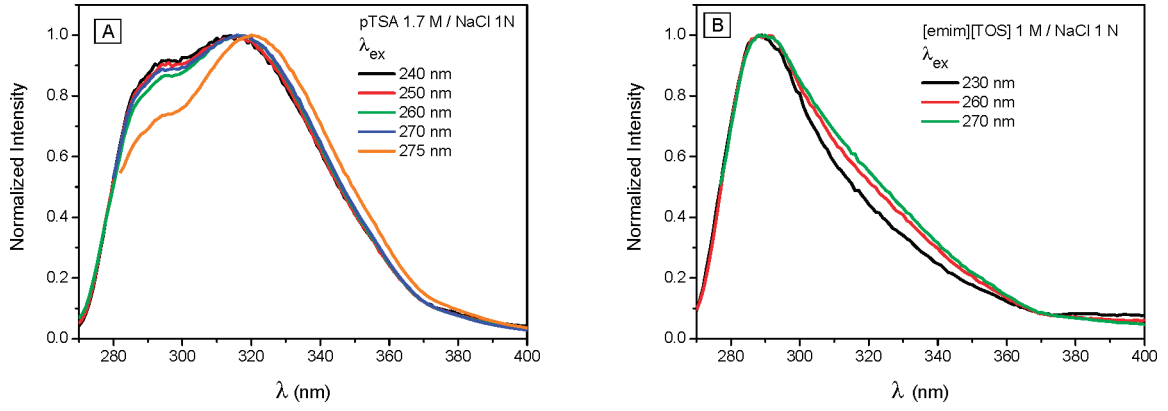

Figure 4. Normalized emission spectra of (A) pTSA and (B) [emim][TOS] dissolved in 1 N NaCl aqueous solution with chromophore concentrations close to 1 M, indicated in the legend. Excitation wavelengths indicated in the legend.

the monomer excited state and that the molecular overlap is only partial in the sandwich-like excimer configuration. The position of the excimer band is common to [emim][TOS] and pTSA, meaning that the steric hindrance to form perfect excimer configurations is not due to the proximity of cations, but to the methyl and sulfonate groups.

Figure 2 shows that excimers of the two compounds are formed at concentrations beyond 0.01 M. The excimer-to-monomer fluorescence ratio of pTSA increases with chromophore concentration above 0.01 M, in deionized water and in 0.1 or 1 N NaCl aqueous solution, and seems to be independent of the NaCl concentration (Figure 2A). In contrast to pTSA, the excimer-to-monomer fluorescence ratio of [emim][TOS] solutions does not grow throughout the whole range of chromophore concentrations, but draws a sigmoid and levels off at about 0.5 M. The different dependence on concentration of the two compounds reveals some differences in the mechanism of excimer formation,

dx.doi.org/10.1021/jp212202b | J. Phys. Chem. B 2012, 116, 3973–3981

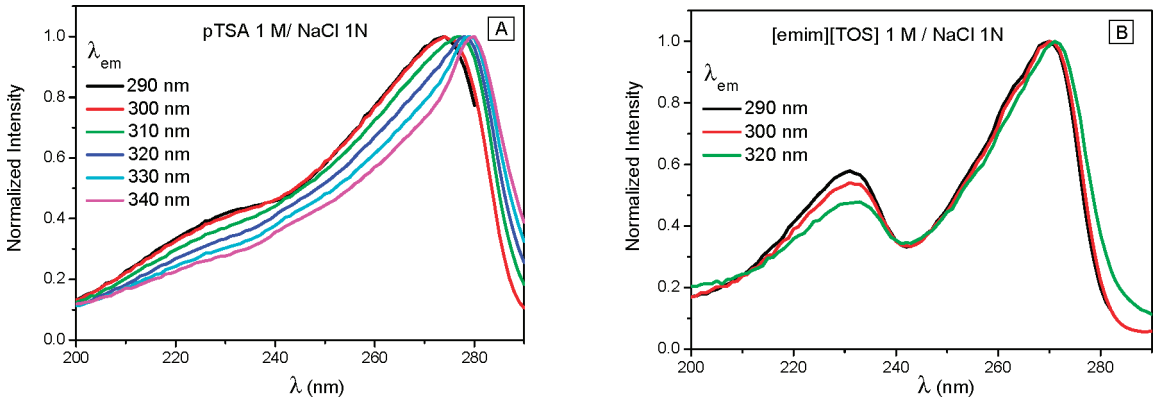

Figure 5. Excitation spectra of (A) pTSA and (B) [emim][TOS] dissolved in 1.0 N NaCl aqueous solution with chromophore concentration 1 M, as indicated in the legend. Emission wavelengths indicated in the legend.

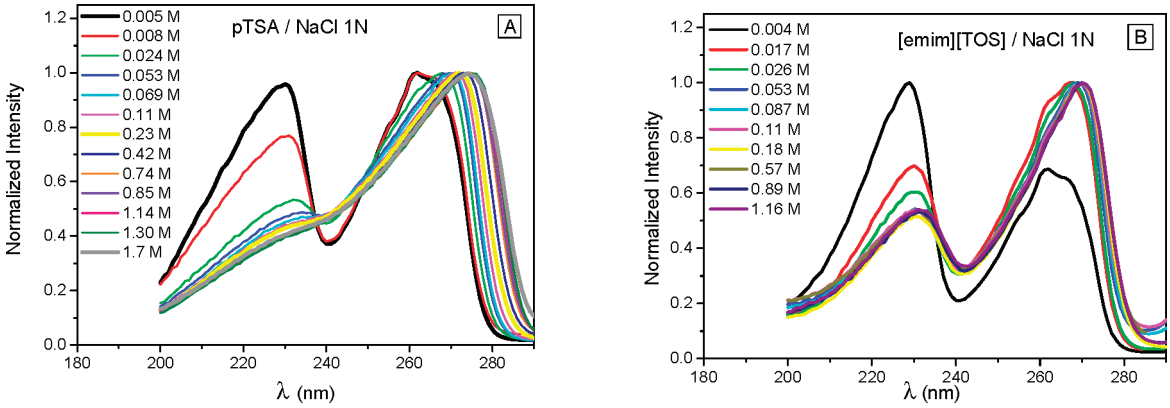

Figure 6. Excitation spectra of (A) pTSA or (B) [emim][TOS] dissolved in 1 N NaCl aqueous solution after filtration. The intensity is normalized to the maximum. Emission wavelength is 300 nm, and chromophore concentrations are indicated in the legend.

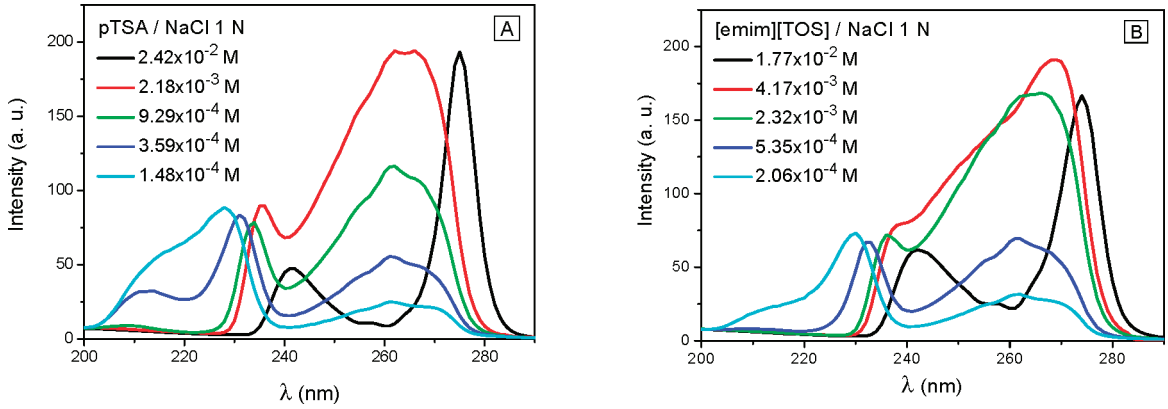

Figure 7. Excitation spectra of (A) pTSA or (B) [emim][TOS] dissolved in 1 N NaCl aqueous solution, without filtration. Emission wavelength is 300 nm, and chromophore concentrations are indicated in the legend.

linked to the cation. Excimers may be formed by diffusion of two *p*-toluenesulfonate groups through a short distance, or by direct absorption of light by pre-existing dimers or aggregates[19,20] and, therefore, the different I_E/I_M values at the larger concentrations could arise from differences in the diffusion and/or aggregation of the two compounds. Let us consider these two possibilities.

The strong acid pTSA is totally dissociated in aqueous media, whereas [emim][TOS] dissolved in deionized water forms ion pairs[16] that, at first sight, might disable excimer formation by slowing chromophore diffusion. The cation−anion proximity, characteristic of ion pairs, can be inferred from the loss of vibrational structure of the absorption spectra of [emim][TOS] at any concentration, with respect to those of pTSA (Figure 3A). This result is consistent with the trend observed in the pairing of like-sized ions (as for [emim][TOS]) in contrast to ions of different size (as pTSA).[21] With increasing NaCl concentration, the absorption spectra of [emim][TOS] retrieve the vibrational resolution (Figure 3B) and become the same as those of pTSA, which remain constant with increasing salt concentration. This suggests that the ionic strength provided by

dx.doi.org/10.1021/jp212202b | J. Phys. Chem. B 2012, 116, 3973−3981

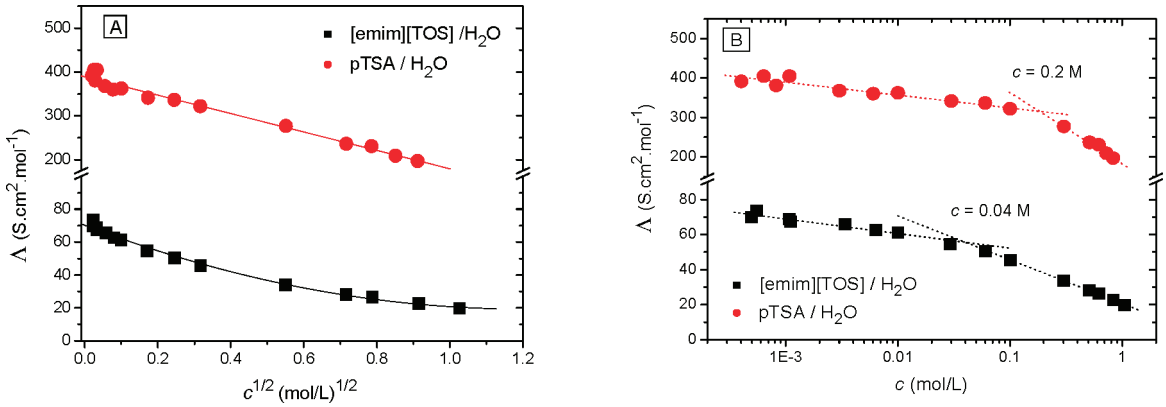

Figure 8. Molar conductivity of [emim][TOS] and pTSA dissolved in deionized water, at 25.0 °C: (A) linear and (B) log plots.

NaCl shields the ionic interactions responsible for [emim]-[TOS] ion pairing.

Nevertheless, ion pair dissociation of [emim][TOS] in 1 N NaCl solutions does not disrupt the plateau of Figure 2B, indicating that the slower diffusion of ion pairs is not responsible for the formation of the plateau.

Let us consider now the relationship between aggregation and excimer formation. The fluorescence ratios of pTSA and [emim][TOS] dissolved in water or in NaCl aqueous solutions depend on the excitation wavelength. Figure 4 shows that excimer emission of tosylate groups in the two compounds changes with excitation wavelength in the range 230−280 nm. Likewise, the excitation spectra depend on the emission wavelength, as shown in Figure 5. These observations are indicative of the existence of multiple absorbing systems, each one having different absorption and emission spectra; i.e., they are indicative of the existence of chromophore aggregates with different sizes or structures. The excitation spectra are in agreement with this conclusion.

Excitation Spectra. Absorption and excitation spectra are expected to be equivalent for single and simple chromophores as tosylate groups. However, unlike the absorption spectra, which show a single band able to cause fluorescence (260 nm, Figure 3), the excitation spectra of pTSA and [emim][TOS] show two or three bands highly dependent in position and relative intensity on chromophore concentration; they do also depend to a lesser extent on the emission wavelength and previous history of the sample, such as filtration (compare Figures 6 and 7). The excitation spectra of monomer emission from dilute solutions (chromophore concentration less than 1×10^{-2} M in filtered solutions and lower in nonfiltered solutions) show a band centered at 260 nm totally coincident with the absorption spectra of chromophores individually dispersed, together with a blue sideband (Figures 6 and 7). With increasing concentration, but below the above limit, the main band at 260 nm of the excitation spectra increases, and the blue sideband shifts to the red. Beyond the concentration limit (1×10^{-2} M in filtered solutions), the excitation and absorption spectra behave differently for both compounds: the absorption spectra do not change in shape with concentration but a new band emerges at the red side of the excitation spectra, the original band at 260 nm diminishes, and the blue and red sidebands shift bathochromically (Figures 6 and 7). Figure 6 shows that, at concentrations above 0.05 M, only the blue and red sidebands (without the band centered at 260 nm) form the excitation spectra; i.e., no longer isolated chromophores are responsible for the emission. The blue and red sidebands should logically be assigned to the absorption of aggregates.

A remarkable difference between pTSA and [emim][TOS] can be observed in Figure 6. Changes in position and relative intensity of the blue and red sidebands of pTSA (Figure 6A) occur in practically the whole range of concentrations, while for [emim][TOS] (Figure 6B), all the spectra are superimposed at concentrations beyond 0.1 M and the blue band is larger in relative intensity and better resolved. It is evident that the evolution of the aggregates structure of both compounds with chromophore concentration is different due to the presence of imidazolium cations, which forces that the structure of [emim][TOS] aggregates remains constant at concentrations above 0.1 M.

In summary, the blue and red sidebands of the excitation spectra denote chromophore aggregation above a certain concentration in any system, [emim][TOS] or pTSA, with or without salt, in filtered or unfiltered solutions. But most chromophores must be molecularly dissolved taking into account that the absorption spectra do not change with concentration. Before discussing in more detail these results, it is necessary to look for assessment on aggregation in other experimental results.

Conductivity Measurements. The specific conductivity (κ) of [emim][TOS] and pTSA aqueous solutions was determined at 25.0 °C as a function of the solute molar concentration (c). Figure 8B shows the molar conductivity ($\Lambda = \kappa/c$, also called equivalent conductivity) plotted versus concentration in the log scale. A double linear behavior with not very marked breaking points at about 0.04 M for [emim][TOS] and 0.2 M for pTSA can be observed. This could be related to a change of the charge carriers, which can be attributed to the formation of less mobile aggregates at concentrations above the breakpoint or cac. The lower cac of the IL suggests that aggregation is enhanced in the case of [emim][TOS] with respect to pTSA.

The molar conductivity of nonassociated systems is expected to follow Kohlrausch's linear dependence on the square root of c

$$\Lambda = \Lambda_0 - \alpha c^{1/2} \quad (1)$$

where Λ_0 is the limit molar conductivity at infinite dilution and α is an empirical constant.

Conductivity data of [emim][TOS] do not follow the linear Kohlrausch's law (Figure 8A), which again is indicative of aggregation. The parameter α depends inversely on the

dx.doi.org/10.1021/jp212202b | J. Phys. Chem. B 2012, 116, 3973−3981

viscosity. Solution viscosity increases with concentration from 0.887 cP for pure water to 1.747 cP for the 1.06 M [emim][TOS] solution in deionized water, at 25.0 °C, a 2-fold increment. Hence, a descent of the slope to half the initial value in the range of concentration from 0 to 1 M may be explained as being due to viscosity, but the slope diminishes more than that (see Figure 8A), suggesting an additional effect that we ascribe to aggregation.

Conductivity measurements provide more evidence for aggregation of [emim][TOS] than for pTSA. Second degree polynomial fit of [emim][TOS] data and linear regression of pTSA data versus $c^{1/2}$ (concentrations above 0.0004 M in both cases) yield Λ_0(pTSA) = 389.4 S·cm^2·mol^{-1} and Λ_0([emim][TOS]) = 70.0 S·cm^2·mol^{-1}. These values of the limit molar conductivity allow determining the corresponding limit molar conductivity of anions and cations, assuming that ions move independently (without forming ion pairs or aggregates) and that, therefore, their limit molar conductivities are additive.

Table 1 summarizes the limit molar conductivity of ions forming part of [emim][TOS] and pTSA. It is well established

Table 1. Limit Molar Conductivity of Ions[a]

ion	Λ_0 (S·cm^2·mol^{-1})	counterion	reference
emim$^+$	30.3	pTS$^-$	this work
	42.91	BF_4^-	24
	53.78	$EtSO_4^-$	24, 25
pTS$^-$	39.7	H$^+$	this work
	39.57	H$^+$	23

[a]The counterions of the compounds whose limit molar conductivity is employed in the calculation are also shown.

that proton limit conductivity in aqueous media at 25.0 °C is $\Lambda_0(H_3O^+)$ = 349.65 S·cm^2·mol^{-1}.[22] With that value and Λ_0(pTSA) here determined, Λ_0 of the pTS$^-$ was calculated, in fairly good agreement with a previously published value[23] (Table 1), which supports the idea that pTSA, at infinite dilution, does not form ion pairs or aggregates in significant amount as to slow down ion diffusion.

From Λ_0(pTS$^-$) and Λ_0([emim][TOS]) it is possible to obtain the limit molar conductivity of the 1-ethyl-3-methylimidazolium cation in water at 25.0 °C: Λ_0(emim$^+$) = 30.3 S·cm^2·mol^{-1}. A larger value (Table 1) determined with tetrafluoroborate (BF_4^-) as counterion was reported,[24] and an even larger value is determined (Table 1) with the experimental Λ_0 value of 1-ethyl-3-methylimidazolium ethylsulfate in water at 25.0 °C (Λ_0([emim][$EtSO_4$]) = 84.05 S·cm^2·mol^{-1})[25] and that of the anion ($\Lambda_0(EtSO_4^-)$ = 30.27 S·cm^2·mol^{-1}).[24] This suggests that ion limit molar conductivity, which reflects ion mobility, is inversely related not only to ion size but also to cation–anion association[2] and to the size of the hydration sphere.[26] While [emim][$EtSO_4$] is fully dissociated in aqueous solution,[25] the present result on Λ_0(emim$^+$) indicates that ion pairing of [emim][TOS] retards cation diffusion in the limit of infinite dilution. Again, it must be concluded that, contrary to pTSA, in the limit of infinite dilution [emim][TOS] forms ionic pairs in salt-free aqueous solution.

Density Measurements. Another magnitude closely related to aggregation is the apparent molar volume (V, in cm^3/mol) determined through density measurements (ρ, in g/cm^3) by means of the following expression

$$V = \frac{M}{\rho} + \frac{10^3}{m}\left[\frac{1}{\rho} - \frac{1}{\rho_0}\right] \quad (2)$$

where ρ_0 represents solvent density, M is the molecular weight of the solute, and m is the molal concentration (mol/kg). Figure 9 shows the apparent molar volume of [emim][TOS]

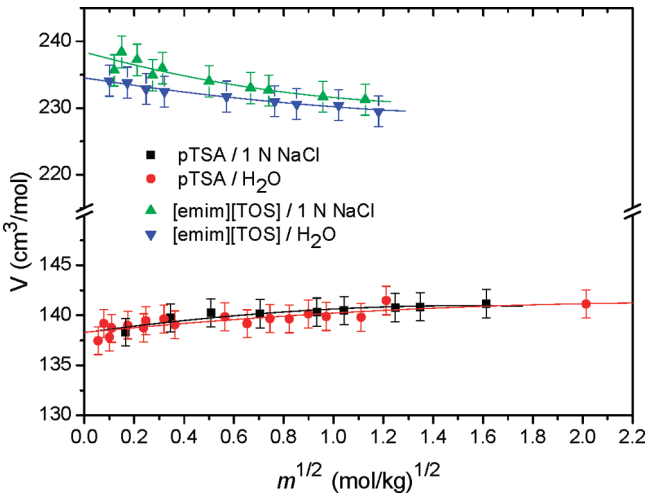

Figure 9. Apparent molar volume of pTSA and [emim][TOS] dissolved in deionized water and in 1 N NaCl aqueous solution at 25.00 °C. Lines are polynomial fits to eq 3. Error bars 1%.

and pTSA in aqueous solutions and in 1 N NaCl aqueous solutions, at 25.00 °C, as a function of the square root of the molality ($m^{1/2}$). V increases slightly with m for pTSA (as observed for aggregating ILs[3] and for surfactants[27]) but follows the opposite trend for [emim][TOS]. The increment of V is commonly assigned to the release of water in the hydration shell of the monomers upon aggregation.[28]

Two linear regions with a breaking point are expected[3] for aggregation in Figure 9 type plots, but it was not observed in plots either versus $1/m$ or versus m or $m^{1/2}$, which are the standard methods employed to determine cac through density measurements. Assuming that the IL and pTSA behave as 1:1 inorganic electrolytes, V values were fitted to the Redlich–Mayer equation[29]

$$V = V^o + Am^{1/2} + Bm \quad (3)$$

where V^o is the apparent molar volume in the limit of infinite dilution; A represents the coefficient of the Debye–Hückel limiting law and amounts[30] to 1.865 cm^3·kg$^{1/2}$·mol$^{-3/2}$ for 1:1 electrolytes in water at 25.0 °C; B is an empirical parameter which can be evaluated by linear regression of $V - Am^{1/2}$ versus m and is equivalent to the second virial coefficient that measures the departure of the ideal system (B = 0) due to nonelectrostatic ion–ion interactions (hydrogen bonds, hydrophobic interactions, π–π interactions, etc.). For ILs in aqueous solution, B is generally negative and its absolute value increases with increasing temperature and chain length of cation substituents, denoting the increased nonelectrostatic interactions.[3,31]

Table 2 summarizes V^o values for [emim][TOS] and pTSA. The effective molar volume of the cation 1-ethyl-3-methylimidazolium ([emim$^+$]) in deionized water at 25.0 °C is 99.20

dx.doi.org/10.1021/jp212202b | J. Phys. Chem. B 2012, 116, 3973–3981

Table 2. Limit Molar Volumes and Second Virial Coefficients at 25.0 °C

compound	solvent	V^o ($cm^3 \cdot mol^{-1}$)	B ($cm^3 \cdot kg \cdot mol^{-2}$)
[emim][TOS]	water	232.8 ± 0.4	−4.4 ± 0.5
	NaCl 1 N	235.8 ± 0.6	−6.3 ± 1.0
pTSA	water	138.4 ± 0.1	−0.2 ± 0.1
	NaCl 1 N	140.1 ± 0.5	−0.9 ± 0.5

cm^3/mol,[32] and therefore, assuming additivity of the cation and anion contributions, the molar volume of the anion tosylate (pTS^-) is 133.6 cm^3/mol and that of the solvated proton of pTSA is 4.8 cm^3/mol, a result not consistent with the formation of aggregates in significant amounts. In 1 N NaCl aqueous solution (Table 2) the apparent molar volume at infinite dilution of both compounds increases slightly, about 1%, which would be compatible with increasing aggregation over deionized water (salting out effect).[28]

Also, Table 2 shows too that the second virial coefficient B is, in absolute value, much larger for [emim][TOS] than for pTSA (because of the larger hydrophobic interactions of the first one) and larger in 1 N NaCl than in deonized water, supporting again a salting out effect. In summary, water is worse solvent for [emim][TOS] than for pTSA, and NaCl aqueous media are worse solvents than water for both compounds. Thus, greater tendency to aggregation should be expected for [emim][TOS] than for pTSA, and in salt media than in pure water, but molar volume data do not provide clear evidence for aggregation, either because aggregates are small and/or because they are in low concentration.

Aggregation-Induced Emission Enhancement. Conductivity measurements support weak aggregation of [emim][TOS] and even weaker of pTSA in aqueous solution, while density measurements indicate that aggregates do not influence significantly the molar volume. Contrarily, according to the excitation spectra the whole emission observed at the larger concentrations seems to be originated solely by the aggregates. These results are seemingly contradictory but they become compatible if we consider aggregation-induced emission enhancement. The small fraction of chromophores forming part of aggregates absorbs in the red and blue edges of the absorption band and their contribution to the absorption spectra is negligible but they are efficiently fluorescent. Aggregation generally quenches the emission. The chromophores that are highly fluorescent in their dilute solutions become weakly luminescent or even nonemissive in solid state when the close vicinity between them induces nonradiative energy transfer, resulting in drastic reduction of the emission intensity. Aggregation-induced emission enhancement is the opposite phenomenon. It is due to different mechanisms such as protection from quenching by solvent molecules, restriction of intramolecular motions, or prevention of parallel staking of chromophores by bulky counterions.[33−37] In the systems here considered, since the chromophore is a simple homocycle, a phenylene group, probably, the rigidity imposed by aggregation inhibits the nonradiative decay and thus enhances the emission. However, the mechanism responsible for the enhancement is not yet known.

Thanks to aggregation-induced emission enhancement, fluorescence is much more sensitive than conductivity or density measurements for detecting aggregation and thereby the structure of aggregates can be studied.

Structure of the Aggregates. It is well-known that, upon increasing concentration, new bands appear at the red and blue sides of the absorption spectra of some dyes in aqueous solution. These spectral changes have long been attributed to the formation of dimers or larger aggregates.[37−41] Here we observe those spectral changes in the excitation spectra, which are equivalent to the absorption spectra. The advantage of excitation spectra with front face excitation, regarding absorption spectra, is that they allow measuring very dilute and very concentrated solutions, covering even six decades of the chromophore concentration.

This behavior of the absorption spectra is characteristic of the formation of head-to-head and head-to-tail aggregates. When two identical chromophores come to close proximity, their exciton coupling causes a shift of the absorption spectrum that depends on the relative dipole orientation. Planar molecules as cyanine dyes tend to form aggregates with parallel arrangement.[39,40] Parallel orientation with head over head (H, face-to-face or sandwich-like aggregates) results in blue shift, head-to-tail orientation on a line (J-aggregates) leads to a red shift, and the intermediate oblique orientation (Scheme 2) produces band splitting with two bands appearing at lower and higher wavelengths.[40] J structures are more exposed to solvent than H ones and therefore the J or H preference of a given molecule depends on the driving force for stabilizing the aggregates. The fluorescence of J-aggregates appears at nearly the same wavelength as the bathochromically shifted narrow and intense absorption peak while H-aggregates are weakly fluorescent or non fluorescent.

Scheme 2. Geometrical Characteristics of Tosylate Assemblies with Intermediate Structures between Those of Pure J- and H-Aggregates

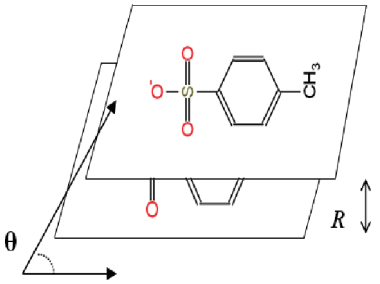

The aggregation of ILs in aqueous solution is well documented,[3,4,8,9] although, as far as we know, this is the first report on a well-defined structure of anion aggregates in assemblies intermediate to those of type H or J. Within this type of clusters the aromatic rings are disposed in parallel planes at an intermolecular distance R and twisted at an angle θ. The slip angle θ is the angle between the line of centers of a stack of molecules and the long molecular axes of any of the parallel molecules (Scheme 2). It is related with the relative values of f_J and f_H, the area under the blue (f_H) and red (f_J) side absorption bands of aggregates.[38] Usually, they are difficult to isolate from the absorption spectra but, fortunately, here they can be identified with the corresponding bands of the tosylate excitation spectra and qualitative descriptions of the evolution of the slip angle with chromophore concentrations can be tempted.

The slip angle changes in the different ranges of tosylate concentration. H-aggregates correspond to $\theta = 90°$ or $f_J/f_H = 0$, and they are observed only in the very dilute solutions with

dx.doi.org/10.1021/jp212202b | J. Phys. Chem. B 2012, 116, 3973−3981

chromophore concentrations below 1×10^{-3} M. In that range, the red sideband, if it exists, is hidden below the absorption of single chromophores (which are predominant) and since its shape is not distorted it seems that it has a negligible intensity with respect to that of the blue sideband. Pure or almost pure H-aggregates should be formed.

Above that concentration, in the range 10^{-3} to 5×10^{-2} M, the red sideband is overlapped with the absorption of single chromophores, leading to a distortion of the last one; f_J/f_H increases from below 1 to above 1 and consequently the tosylate groups tilt progressively tending to align each other with $\theta = 0°$.

Only pTSA form almost pure J-aggregates ($f_H \approx 0$) at concentrations above 5×10^{-1} M; [emim][TOS] is not able to do it. The aggregates of tosylate in the IL tilt to a certain limit angle (a maximum f_J/f_H, minimum θ) logically imposed by the proximity of cations arranged around anions, whether or not incorporated in the space between molecular planes in the aggregate.[40] Beyond 5×10^{-2} M the structure of pTSA aggregates keeps evolving in the same way as before (red shift of the red sideband and increasing f_J/f_H) but that of the IL aggregates remains frozen in the same minimum θ value.

CONCLUSIONS

This work studies the formation of ionic pairs and aggregates of the IL [emim][TOS] and its model compound, pTSA, in aqueous media with and without salt. The model compound is totally dissociated in any studied condition but [emim][TOS] dissolved in deionized water and in 0.1 N NaCl forms ion pairs, which dissociate in the presence of high NaCl concentrations (1 N).

The existence of aggregates is controversial at first sight because several apparently contradictory results were obtained with different techniques. Conductivity measurements support the existence of aggregates in [emim][TOS] and pTSA aqueous solutions, and show a larger trend to aggregation of [emim][TOS] than pTSA, when dissolved in deionized water.

On the other hand, the apparent molar volume measurements, although slightly larger in 1 N NaCl aqueous solution than in deionized water, do not provide clear evidence for the aggregation of [emim][TOS] and pTSA in aqueous solution or in salt aqueous solutions. This is likely because aggregates are small in size and/or their concentration is low. However, according to values of the second virial coefficient, more aggregates should be expected for [emim][TOS] than for pTSA, and in 1 N NaCl aqueous solution than in deionized water.

Finally, the existence of aggregates of [emim][TOS] and pTSA in aqueous solution, with or without salt, becomes clearly evident through the excitation and emission spectra of the tosylate intrinsic fluorescence. All these results are reconciled with each other, when taking into account aggregation-induced emission enhancement, which means that the fluorescence quantum yield of aggregated chromophores is much larger than for chromophores individually dissolved, and therefore, despite the low abundance of chromophore aggregates, they get the largest part of the emission.

According to the shape of the excitation spectra, it appears that aggregates are formed by tosylate groups arranged in parallel stacks twisted at a slip angle that, increasing concentration, changes from 90° (H or head-to-head configuration) to 0° (J or head-to-tail configuration) for pTSA, while for [emim][TOS] it decreases from 90° to a minimum slip angle (larger than 0°) that, once attained, remains constant because imidazolium cations prevent the pure head-to-tail configuration of anions.

In brief, aggregation is driven by anion−anion interactions, anion concentration determines the slip angle, cations control the minimum slip angle, and salt concentration is responsible for the disappearance of ionic pairs and for the salting-out effect on the trend to aggregation.

AUTHOR INFORMATION

Corresponding Author

*E-mail: ipierola@ccia.uned.es. Phone: 34-91-3987376. Fax: 34-91-3987390.

Notes

The authors declare no competing financial interest.

ACKNOWLEDGMENTS

This work received financial support from the "Ministerio de Ciencia e Innovación" (Spain) under grant CTQ2010-16414/BQU and from the "Comunidad Autónoma de Madrid" under grant S2009/ESP1691.

REFERENCES

(1) Wasserscheid, P., Welton, T., Eds. *Ionic Liquids in Synthesis*, 2nd ed.; VCH-Wiley: Weinhein, Germany, 2008.
(2) Tokuda, H.; Hayamizu, K.; Ishii, K.; Susan, M. A. B. H.; Watanabe, M. *J. Phys. Chem. B* **2004**, *108*, 16593−16600.
(3) Wang, J.; Wang, H.; Zhang, Sh.; Zhang, H.; Zhao, Y. *J. Phys. Chem. B* **2007**, *111*, 6181−6188.
(4) Bowers, J.; Butts, C. P.; Martin, P. J.; Vergara-Gutierrez, M. C. *Langmuir* **2004**, *20*, 2191−2198.
(5) Dorbritz, S.; Ruth, W.; Kragl, U. *Adv. Synth. Catal.* **2005**, *347*, 1273−1279.
(6) Singh, T.; Kumar, A. *J. Phys. Chem. B* **2008**, *112*, 4079−4086.
(7) Zhao, Y.; Gao, S.; Wang, J.; Tang, J. *J. Phys. Chem. B* **2008**, *112*, 2031−2039.
(8) Blesic, M.; Lopes, A.; Melo, E.; Petrovski, Z.; Plechkova, N. V.; Lopes, J. N. C.; Seddon, K. R.; Rebelo, L. P. N. *J. Phys. Chem. B* **2008**, *112*, 8645−8650.
(9) Dong, B.; Gao, Y.; Su, Y.; Zheng, L.; Xu, J.; Inoue, T. *J. Phys. Chem. B* **2010**, *114*, 340−348.
(10) Vanyur, R.; Biczok, L.; Miskolczy, Z. *Colloids Surf., A* **2007**, *299*, 256−261.
(11) Fei, Z.; Zhu, D.-R.; Yang, X.; Meng, L.; Lu, Q.; Ang, W. H.; Scopelliti, R.; Hartinger, Ch. G.; Dyson, P. J. *Chem.—Eur. J.* **2010**, *16*, 6473−6481.
(12) Shi, L.; Li, N.; Yan, H.; Gao, Y.; Zheng, L. *Langmuir* **2011**, *27*, 1618−1625.
(13) Paul, A.; Mandal, P. K.; Samanta, A. *Chem. Phys. Lett.* **2005**, *402*, 375−379.
(14) Zhang, J.; Zhang, Q.; Shi, F.; Zang, Sh.; Qiao, B.; Liu, L.; Ma, Y.; Deng, Y. *Chem. Phys. Lett.* **2008**, *461*, 229−234.
(15) Chen, X. W.; Liu, J. W.; Wang, J. H. *J. Phys. Chem. B* **2011**, *115*, 1524−1530.
(16) Pierola, I. F.; Pacios, I. E. *J. Fluoresc.* **2012**, *22*, 145−150.
(17) Freire, M. G.; Neves, C. M. S.; Silva, A. M. S.; Santos, L. M. N. B. F.; Marrucho, I. M.; Rebelo, L. P. N; Shah, J. K.; Magin, E. J.; Coutinho, A. P. *J. Phys. Chem. B* **2010**, *114*, 2004−2014.
(18) Wang, H.; Feng, Q.; Wang, J.; Zhang, H. *J. Phys. Chem. B* **2010**, *114*, 1380−1387.
(19) Salom, C.; Semlyen, J. A.; Clarson, S.; Hernandez-Fuentes, I.; Maçanita, A. L.; Horta, A.; Pierola, I. F. *Macromolecules* **1991**, *24*, 6827−6831.
(20) Dias, F. B.; Lima, J. C.; Pierola, I. F.; Horta, A.; Maçanita, A. L. *J. Phys. Chem. A* **2001**, *105*, 10286−10295.

(21) Lund, M.; Jagoda-Cwiklik, B.; Woodward, C. E.; Vacha, R.; Jungwirth, P. *J. Phys. Chem. Lett.* **2010**, *1*, 300−303.
(22) *CRC Handbook of Chemistry and Physics*, 78th ed.; Lide, D. R., Ed.; CRC Press: Boca Raton, FL, 1997−1998.
(23) Bhat, V. S.; Srivastava, A. K. *J. Chem. Eng. Data* **2001**, *46*, 1215−1221.
(24) Wong, Ch.-L.; Soriano, A. N.; Li, M.-H. *Fluid Phase Equilib.* **2008**, *271*, 43−52.
(25) Bester-Rogac, M.; Hunger, J.; Stoppa, A.; Buchner, R. *J. Chem. Eng. Data* **2011**, *56*, 1261−1267.
(26) Anouti, M.; Jones, J.; Boisset, A.; Jacquemin, J.; Caillon-Caravanier, M.; Lemordant, D. *J. Colloid Interface Sci.* **2009**, *340*, 104−111.
(27) Zielinski, R.; Ikeda, S.; Nomura, H.; Kato, S. *J. Chem. Soc., Faraday Trans. 1* **1988**, *84*, 151−163.
(28) Milioto, S.; Causi, S.; De Lisi, R. *J. Solution Chem.* **1993**, *22*, 1−26.
(29) Redlich, O.; Mayer, D. M. *Chem. Rev.* **1964**, *64*, 221−227.
(30) Ananthaswamy, J.; Atkinson, G. *J. Chem. Eng. Data* **1984**, *29*, 81−87.
(31) Shekaari, H.; Mansoori, Y.; Sadeghi, R. *J. Chem. Thermodyn.* **2008**, *40*, 852−859.
(32) Costa, A. J. L.; Esperança, J. M. S. S.; Marrucho, I. M.; Rebelo, L. P. N. *J. Chem. Eng. Data* **2011**, *56*, 3433−3441 and references therein..
(33) Gao, B.-R.; Wang, H.-Y.; Hao, Y.-W.; Fu, L.-M.; Fang, H.-H.; Jiang, Y.; Wang, L.; Chen, Q.-D.; Xia, H.; Pan, L.-Y.; Ma, Y.-G.; Sun, H.-B. *J. Phys. Chem. B* **2010**, *114*, 128−134.
(34) Feng, X.; Tong, B.; Shen, J.; Shi, J.; Han, T.; Chen, L.; Zhi, J.; Lu, P.; Ma, Y.; Dong, Y. *J. Phys. Chem. B* **2010**, *114*, 16731−16736.
(35) Lamere, J. F.; Saffon, N.; Dos Santos, I.; Fery-Forgues, S. *Langmuir* **2010**, *26*, 10210−10217.
(36) Hong, Y.; Lam, J. W. Y.; Tang, B. Z. *Chem. Commun.* **2009**, 4332−4353.
(37) Luo, J.; Xie, Z.; Lam, J. W. Y.; Cheng, L.; Chen, H.; Qiu, C.; Kwok, H. S.; Zhan, X.; Liu, Y.; Zhu, D.; Tang, B. Z. *Chem. Commun.* **2001**, 1740−1741.
(38) Lopez-Arbeloa, F.; Martinez-Martinez, V.; Bañuelos-Prieto, J.; Lopez-Arbeloa, I. *Langmuir* **2002**, *18*, 2658−2664.
(39) Emerson, E. S.; Conlin, M. A.; Rosenoff, A. E.; Norland, K. S.; Rodriguez, H.; Chin, D.; Bird, G. R. *J. Phys. Chem.* **1967**, *71*, 2396−2403.
(40) West, W.; Pearce, S. *J. Phys. Chem.* **1965**, *69*, 1894−1903.
(41) Sasai, R.; Iyi, N.; Fujita, T.; López-Arbeloa, F.; Martínez-Martínez, V.; Takagi, K.; Itoh, H. *Langmuir* **2004**, *20*, 4715−4719.